Influence of biaxial stress on magnetostriction-Experiments and modeling

Olivier Hubert, Z. Maazaz, J. Taurines, R. Crepinge, F. van den Berg, C. Celada-Casero

Influence of biaxial stress on magnetostriction - experiments and modeling

O. Hubert[a,*], Z. Maazaz[a], J. Taurines[a], R. Crepinge[a], F. van den Berg[b], C. Celada-Casero[b]

[a] *Université Paris-Saclay, CentraleSupélec, ENS Paris-Saclay, CNRS, LMPS laboratoire de Mécanique, 4 avenue des sciences, Gif-sur-Yvette, 91190, France*
[b] *Tata Steel, PO-Box 10.000, IJmuiden, 1970CA, The Netherlands*

Abstract

The paper deals with the influence of biaxial stress on the magnetic and magnetostriction behavior of a low carbon steel used for structural pieces in the car industry. Material, specimen, measurement set-up and protocol are presented. Anhysteretic measurements are performed, giving results in accordance with literature. A quadratic approximation of magnetostriction vs. induction measurements allows the evaluation of a single magnetostriction parameter per mechanical state. Results are compared to the outputs of a multiscale model, which indicate coherent tendencies but some significant amplitude differences.

Keywords: biaxial mechanical loading, magnetostriction, low carbon steel,

Introduction

In the last few years, a growing interest of the car industry for the use of Advanced High Strength Steel (AHSS) products has been observed, especially considering the weight saving solutions they lead to. Their excellent mechanical behavior comes from the very complex microstructure they exhibit, achieved thanks to precise thermomechanical treatments. The AHSS microstructure is highly sensitive to small variations in the forming process, and it is the purpose of developments in online non-destructive evaluation to detect these minor variations. Such monitoring is made on laminations usually subjected to multiaxial mechanical stress (due to band tension or bending on cylinders) and known to have a strong effect on the magnetic behavior. Stresses can therefore modify the perception of the microstructure given by the sensors. Magnetomechanics must consequently be taken into account in the reverse identification process and requires developing multiaxial experiments and multiaxial magneto-mechanical models. Previous works have addressed magnetic behavior change due to multiaxial stress [1, 2, 3, 4]. In this study, some new results showing the effect of a biaxial stress on the magnetostrictive behavior are presented.

1. Protocol

The material considered in this study is a hot-rolled low carbon (0.08wt%C - 0.35wt%Mn) steel (thickness 3.7mm) provided by Tata Steel. The post hot-rolled state ensures an isotropic global magnetic and mechanical behaviors in accordance with a low crystallographic texture and fine equiaxis grains structure as illustrated by Figure 1. The material is mainly single-phased (b.c.c. ferrite) with very few perlite islands (some dark areas in Figure 1a).

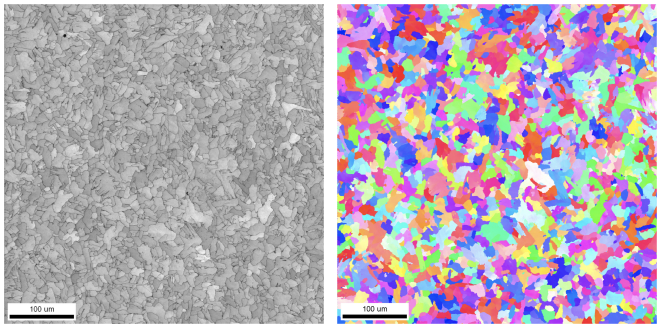

(a) IQ (b) IPF - ND

Figure 1: Microstructure observed by electron back-scattered diffraction: (a) Image Quality mapping ; (b) Inverse pole figure (OIM software)

The experimental protocol associated with biaxial experiments has already been detailed in other publications for magnetic measurement [2]. A new procedure applies for magnetostriction measurement. Experiments are carried using a cross-shaped specimen (Figure 2) designed to promote homogeneous stress and magnetic field in the central area [5]. The local stress tensor (σ_1,σ_2) is related to applied forces (F_1, F_2) by an interacting matrix following:

$$\begin{pmatrix} \sigma_1 \\ \sigma_2 \end{pmatrix} = \begin{pmatrix} \alpha_{11} & \alpha_{12} \\ \alpha_{21} & \alpha_{22} \end{pmatrix} \begin{pmatrix} F_1 \\ F_2 \end{pmatrix} \quad (1)$$

Parameters α_{ij} of this matrix have been numerically calculated by finite element modeling (Figure 2b) using linear elasticity and conventional stiffness (Young modulus 200GPa) and Poisson ratio (0.3) for steel. Due to symmetry and isotropy of the material, the following parameters have been obtained: α_{11}= α_{22}=4.0 MPa/kN and α_{12}=α_{21}=-0.89 MPa/kN (values have been experimentally verified). The mechanical calculation also demonstrates that compression can be applied without risk of buckling. Stress concentrations are however observed in some places. Considering the yield stress of the material

*olivier.hubert@ens-paris-saclay.fr

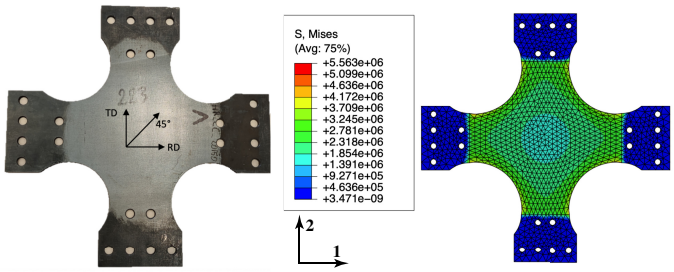

Figure 2: Cross shaped specimen and finite element calculation representing the von-mises equivalent stress ($F_1 = F_2$=500N) - arrows (1,2) indicate the specimen frame and directions of applied forces.

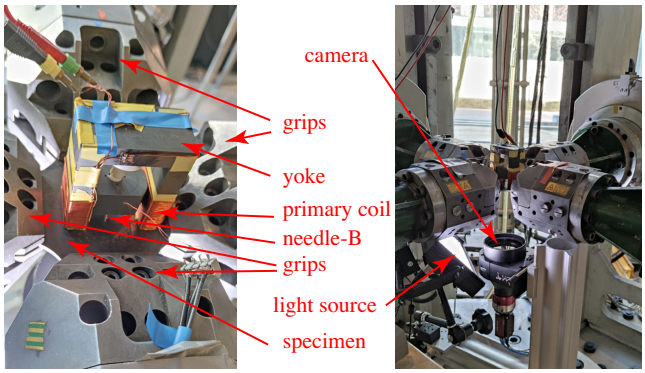

Figure 3: Left: detail of the magnetic measurement set-up; right: positioning inside biaxial machine, camera and light source for DIC.

(250MPa previously measured using uniaxial test), the central mechanical loading amplitude cannot exceed 100MPa.

As illustrated in Figure 3 left, the magnetic field is generated thanks to a ferrimagnetic U-yoke placed on the upper surface and wound with 100 turns. A needle-B is placed between the arms of the yoke to measure the magnetic induction. Magnetic field is evaluated from the current in the primary winding using Ampere's law and a correcting demagnetizing factor (evaluated from finite element magnetostatic modeling of the set-up). Considering the strong non-linearity which can exist between the magnetic field and the current, we mainly focus on the magnetic behavior at low field. Longitudinal (parallel to the applied field) and transversal (perpendicular to applied field) non-magnetoresistive gauges have been stuck in the middle of the specimen between the needles to measure magnetostriction (see reference [6] for more details). Figure 3 right gives a global view of set-up, specimen, grips and hydraulic actuators. Camera and light source are visible, enabling digital image correlation (DIC) of lower sample surface to ensure the proper conduct of mechanical test (see [7] for more details).

The experimental procedure consists to: i) clamp the specimen in the multiaxial machine (Figure 3) and put the magnetic set-up; ii) apply the mechanical loading (σ_1, σ_2) and equilibrate the wheatstone bridges just after to avoid their saturation; iii) demagnetize the material by applying a sinusoidal magnetic field of decreasing amplitude up to zero; iv) perform low frequency magnetic hysteresis (0.2Hz) and anhysteretic measurements [8]. Results presented in this paper are limited to anhysteretic behaviors carried out along the rolling direction of the sheet (corresponding to axis 1 in Figure 2). 25 biaxial (σ_1,σ_2) stress states have been tested, for stress level varying between -100MPa and +100MPa. For an easier comment, the following mechanical loading types are defined: *Longitudinal* tests correspond to situations where $\sigma_1 \neq 0$ and σ_2=0; *Transversal* tests correspond to σ_1=0 and $\sigma_2 \neq 0$; *Equibiaxial* tests mean σ_1=σ_2; and *Shear* tests verify σ_1=-σ_2). Plotting a scalar value representative of a magnetic quantity in the biaxial plane (σ_1,σ_2) is another efficient solution to appreciate the effect of mechanical loading.

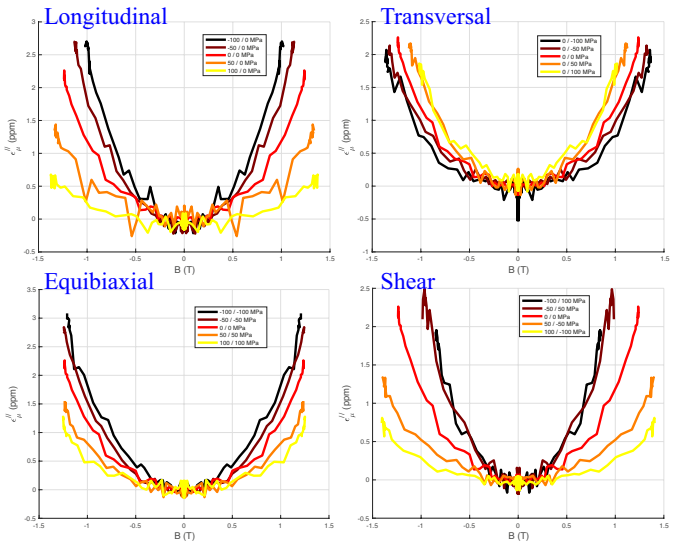

Figure 4: Influence of various stress states and amplitude on the anhysteretic magnetostriction (deformation measured in the direction of applied field).

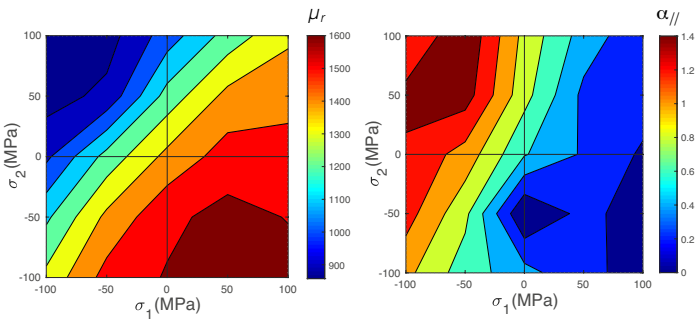

Figure 5: Experiments: biaxial stress influence on (a) initial anhysteretic relative permeability μ_r; (b) magnetostriction sensitivity parameter $\alpha_{//}$ for magneostriction along applied field.

2. Experimental results

Figure 5a gives a map representation of biaxial stress influence on initial anhysteretic permeability recorded for the 25 loading states and interpolated, allowing for an easy visualization of gradients and isovalues. Concerning *Longitudinal* tests, it is observed that tension increases the permeability whereas compression decreases it; an opposite effect is observed for *Transversal* tests; the magnetic permeability looks insensitive

to *Equibiaxial* loading in the range of experiments; a *Shear* loading leads to the most significant changes: permeability increases when stress in the direction of applied field (σ_1) is positive, it decreases when negative.These results are roughly in accordance with previous results reported in [3] for a DP steel and in [8] for an iron-cobalt alloy. Figure 4 plots the anhysteretic longitudinal magnetostriction (along the magnetic field direction) measured for the same stress situations as previously defined. Curves exhibit a parabolic shape and stress state has en effect on apparent amplitude of each curve. It must be recalled that magnetostriction is artificially taken as 0 at B=0 (the initial magnetostriction is unknown). Figure 6 allows for a comparison of reference longitudinal and transversal magnetostriction results obtained with a long strip and placed in a 1D measurement bench (without mechanical loading) with magnetostriction measured with the biaxial set-up at zero applied stress. Amplitudes are significantly lower in the present study, which is mainly explained by a low induction level due to set-up limitation. Concerning *Longitudinal* tests, we observe that tension decreases the magnetostriction amplitude whereas compression increases it. This result is in accordance with observations reported in literature [8, 9]. An opposite effect is observed for *Transversal* tests. Amplitude variations are however significantly lower. Although magnetic behavior looks insensitive to *Equibiaxial*, magnetostriction variations joint the variations observed for *Longitudinal* loading with a smaller amplitude. *Shear* loading leads to the most significant changes of the magnetostriction behavior as for the magnetic behavior: magnetostriction amplitude decreases when stress component in the direction of applied field (σ_1) is positive; it decreases when negative. This is the first time to our knowledge that magnetostriction measurements of *Transversal*, *Equibiaxial* and *Shear* situations are published. In order to adopt a level representation like in Figure 5a, we wish to identify a scalar value representative of each characteristic. Among the possibilities, we propose to perform an approximation of each curve by an even polynomial of degree 4 in B within induction range of ±1T and to retain the 2nd degree value (this polynomial form was originally introduced by Jiles [10]). This gives:

$$\epsilon^{\mu}_{//} = \alpha_{//} B^2 + \beta_{//} B^4 \quad \text{with} \quad \alpha_{//} = \frac{1}{2} \left. \frac{d^2 \epsilon_{\mu}}{dB^2} \right|_{B=0} \tag{2}$$

Figure 5b gives a map representation of biaxial stress influence on $\alpha_{//}$ parameter optimized for the 25 loading states and interpolated, allowing for an easy visualization of gradients and isovalues. It can be observed that isovalues slopes are close to each other in the measurement range. They look different from isovalues slopes for anhysteretic permeability, leading to a higher influence of stress applied along the magnetization direction. The interpretation usually proposed for magnetostriction is based on the evolution of the magnetic domain structure under stress [8, 9]. For iron and steels, uniaxial traction generally decreases the magnitude of magnetostriction. When a perpendicular compression is superimposed, it looks relevant that effect is accentuated. Uniaxial compression has an opposite effect. The superposition of a perpendicular traction leads to an increase of magnetostriction amplitude (and therefore of parameter $\alpha_{//}$). It seems difficult, however, to push the interpretation further. Some comparisons with outputs of a multiscale model tested for several years is proposed in the following section.

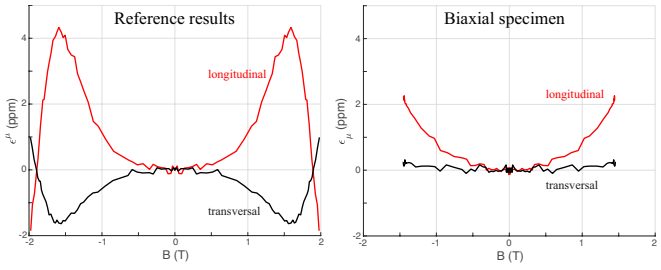

Figure 6: Comparison between magnetostriction measured by 1D frame and 2D set-up - without applied stress

3. Multiscale modeling

The multiscale model (MSM) allows for a reversible description of the magneto-elastic behavior of magnetic materials [11, 12]. Scales involved are the family domain scale α, the grain (crystal) scale g and the representative volume element *RVE* (polycrystal) scale composed of a large number of grains. The Gibbs free energy density is written at the domain scale where magnetization $\mathbf{M}_\alpha$ and magnetostriction strain $\boldsymbol{\varepsilon}^{\mu}_{\alpha}$ can be considered as homogeneous. They are defined as follows:

$$\mathbf{M}_\alpha = M_s \, \gamma^{\alpha}_{k} . \mathbf{e}_k \tag{3}$$

$$\boldsymbol{\varepsilon}^{\mu}_{\alpha} = \frac{3}{2} \begin{pmatrix} \lambda_{100}(\gamma_1^2 - \frac{1}{3}) & \lambda_{111}\gamma_1\gamma_2 & \lambda_{111}\gamma_1\gamma_3 \\ \lambda_{111}\gamma_1\gamma_2 & \lambda_{100}(\gamma_2^2 - \frac{1}{3}) & \lambda_{111}\gamma_2\gamma_3 \\ \lambda_{111}\gamma_1\gamma_3 & \lambda_{111}\gamma_2\gamma_3 & \lambda_{100}(\gamma_3^2 - \frac{1}{3}) \end{pmatrix} \tag{4}$$

M_s is the saturation magnetization and γ^{α}_{k} are the direction cosines of magnetization vector ($\mathbf{e}_k$ is the canonical basis of cubic symmetry). In the framework of linear magnetoelasticity $\boldsymbol{\varepsilon}^{\mu}_{\alpha}$ is the stress independent isovolume magnetostriction tensor where λ_{100} and λ_{111} are two so-called cubic magnetostriction constants. Considering on the other hand stress $\boldsymbol{\sigma}$ and magnetic field $\mathbf{H}$ as homogeneous over the *RVE*, the Gibbs free energy density at the magnetic domain scale writes:

$$\mathfrak{g}_\alpha(\mathbf{H}, \boldsymbol{\sigma}) = K_1(\gamma_1^2\gamma_2^2 + \gamma_2^2\gamma_3^2 + \gamma_3^2\gamma_1^2) - \mu_0 \mathbf{H}.\mathbf{M}_\alpha - \boldsymbol{\sigma} : \boldsymbol{\varepsilon}^{\mu}_{\alpha} \tag{5}$$

μ_0 is the vacuum magnetic permeability and K_1 the first magnetocrystalline constant. The Gibbs free energy density defines 6 minima for $K_1 > 0$, that correspond to iron alloys easy magnetic axes. A minimization of $\mathfrak{g}_\alpha$ with respect to direction cosines of domain families α model the magnetization rotation, and magnetic domains volume fraction f_α is calculated using a Boltzmann function referring to an *at equilibrium* process:

$$f_\alpha = \frac{\exp(-A_s \mathfrak{g}_\alpha)}{\sum_{i=1}^{6} \exp(-A_s \mathfrak{g}_i)} \quad , \quad \boldsymbol{\gamma}_\alpha = min(\mathfrak{g}_\alpha(\boldsymbol{\gamma}, \mathbf{H}, \boldsymbol{\sigma})) \tag{6}$$

with $A_s = 3\chi_0/(\mu_0 M_s^2)$ where χ_0 is the initial stress-free susceptibility. Averaging operations (equation (7)) allows for the

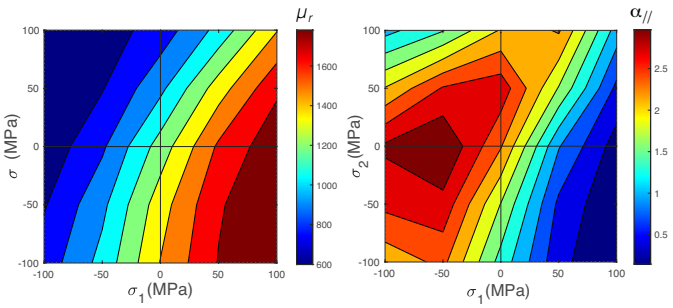

Figure 7: Modeling results: biaxial stress influence on (a) initial anhysteretic relative permeability; (b) magnetostriction sensitivity parameter $\alpha_{//}$.

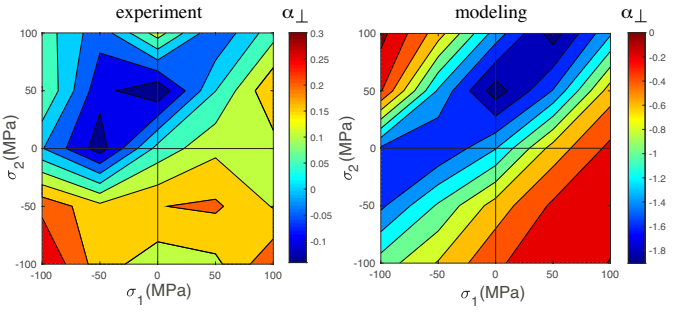

Figure 8: Influence of stress on transversal magnetostriction sensitivity parameter $\alpha_{\perp}$ - comparison between experiment and modeling

calculation of average magnetization and magnetostriction. N_g indicates the number of grains g involved in the process:

$$\mathbf{M} = \frac{1}{N_g}\sum_g\left(\sum_{\alpha=1}^{6} f_\alpha \mathbf{M}_\alpha\right) \quad , \quad \boldsymbol{\varepsilon}^{\mu} = \frac{1}{N_g}\sum_g\left(\sum_{\alpha=1}^{6} f_\alpha \boldsymbol{\varepsilon}_\alpha^{\mu}\right) \qquad (7)$$

An orientation data file made of 250 grains representative of IPF plotted in Figure 1 has been used for the modeling and table 1 gathers the parameters used (all are well-known physical constants of iron [11]; only χ_0 is estimated from experimental magnetization at zero applied stress). Magnetization and magnetostriction have been model using the same magnetic field and stress field ranges as for experiments. Initial anhysteretic permeability and magnetostriction sensitivity parameter $\alpha_{//}$) have been evaluated following the same rules as for experiments. Figure 7 shows a map representation of biaxial stress influence on (a) initial anhysteretic permeability; (b) magnetostriction sensitivity parameter $\alpha_{//}$ calculated from the MSM. The main trends are reproduced by the model for $\sigma_2 > 0$. For $\sigma_2 < 0$, the slope of the modeled permeability isovalues seems more pronounced. The model defines an area where the magnetostriction parameter $\alpha_{//}$ is maximum (for a compression of about -70MPa). This maximum is observed in experiments too but shifted by σ_2=+50MPa approximately. Figure 8 shows the evolution of the magnetostriction parameter $\alpha_{\perp}$ obtained for magnetostriction deformation perpendicular to the magnetic field. Model and experimental amplitudes are significantly different but tendencies are in accordance especially regarding the occurrence of an area with minimum amplitude, consistent with the 50MPa shift along σ_2 observed for longitudinal magnetostriction. Thus, although, variations of the experimental quantities are in agreement with the MSM, amplitudes and reference position in the stress plane are different: these differences can traduce a modeling that involves too many simplifications. An unbalanced distribution of domains inherited from forming process as can be seen in other materials [4] can be incriminated too.

Table 1: Parameters used for multiscale modeling

M_s (A/m)	K_1 (kJ.m^{-3})	λ_{100}; λ_{111} (ppm)	χ_0
1.71 ×10^6	48	21;-21	1200

Conclusion

In this paper, longitudinal and transversal magnetostriction measurements obtained under biaxial stress of a low carbon steel were presented. They are completed by initial anhysteretic permeability measurements. The experimental results are globally in agreement with the results of a multiscale model. Discrepancies may have a modeling or experimental origin: indeed MSM involves several steps of simplification including an assumption of initial balance of magnetic domains distribution. Residual stresses effect from forming process or occurring during experiments is another possible explanation. For future experiments, the intention is to improve the experimental conditions by increasing the induction level to enhance magnetostriction amplitude (using for example a second yoke) and by implementing a local magnetic field measurement.

Acknowledgements

The work has been developed within the project "Online Microstructure Analytics": Ref. OMA, Grant Agreement No. 847296, Research Fund for Coal and Steel of the European Union.

References

[1] J. Pearson, P.T. Squire, M.G. Maylin, and J.G. Gore. *IEEE Transactions on Magnetics*, 2000.
[2] O. Hubert. *Przeglad Elektrotecniczny*, 83(4):70–77, 2007.
[3] O. Hubert, F.S. Mballa-Mballa, S. He, and S. Depeyre. *IEEE Transactions on Magnetics*, 52(5):1–4, 2016.
[4] U. Aydin et al. *Journal of Magnetism and Magnetic Materials*, 469:19–27, 2019.
[5] O. Hubert et al. *Przeglad Elektrotecniczny*, R81(5):19–23, 2005.
[6] O. Hubert, L. Daniel, and R. Billardon. *Journal of Magnetism and Magnetic Materials*, 254-255(1):352–354, 2003.
[7] M. Rekik, O. Hubert, and L. Daniel. *International Journal of Applied Electromagnetics and Mechanics*, 44(3-4):301–315, 2014.
[8] O. Hubert and L. Daniel. *Journal of Magnetism and Magnetic Materials*, 323(13):1766–1781, 2011.
[9] T. Yamasaki, S. Yamamoto, and M. Hirao. *NDT & E International*, 29(5):263–268, 1996.
[10] D C Jiles. *Journal of Physics D: Applied Physics*, 28(8):1537, 1995.
[11] L. Daniel, O. Hubert, N. Buiron, and R. Billardon. *Journal of the Mechanics and Physics of Solids*, 58(3):1018–1042, 2008.
[12] O. Hubert. *Journal of Magnetism and Magnetic Materials*, 491:165564, 2019.